

Exploring the Concept of a Solar-Battery Car with Single and Double Solar-Trailers

Najib A. Kasti

Department of Mechanical Engineering, Taibah University, Saudi Arabia¹

najib01@idm.net.lb

Abstract-Solar energy is a clean source of energy that is available throughout the year in some parts of the globe. For solar energy to be significant, a large area is needed to harvest solar radiation. One type of machine that attempts to use solar energy, in addition to battery power, is the solar car. Solar cars, used in international competitions, are based on building an efficient system on all fronts (mechanical, aerodynamic, solar panels, batteries, etc.) in order to achieve high speeds and the shortest travel times, while saving consumable energy. At the other extreme of this spectrum of solar-battery cars is a specialized class that attempts to minimize the use of battery power and maximize acquired solar energy. One way to accomplish this is by increasing the size of the solar array.

This paper explores the possible use of solar trailers to increase solar power input. The resulting excess power, derived from solar trailers, may be used to drive accessories that may be life necessities in some parts of the world. At least three variables determine the operating boundaries of solar cars: the net energy produced, the speed of the car and the stability requirements, such as dynamics control and sliding. This paper analyzes these three variables and how they affect the possible use of one/two solar-trailers with solar battery cars.

First, we provide an example that compares the energy consumed by a standalone car and a car with one or two solar-trailers, when traveling along a specific track at different speeds. Next, we analyze the stability of the lateral dynamics using a line model of the car-trailer system at different speeds and various car configurations. Finally, we evaluate the requirements for ground adhesion when travelling along a curved path.

Keywords- Solar Energy; Solar Car; Solar Trailers

I. INTRODUCTION

Gasoline has been powering cars and other machines for an extended period of time. However, such a source may not last indefinitely. In addition, one cannot ignore the adverse effects on the atmosphere caused by the burning such substances. All of these reasons have led humans to seek complementary sources of energy that are free, readily available, nonperishable, and simultaneously friendly to the atmosphere. Solar energy is considered to be a clean, abundant energy. Thus, a class of cars has been designed that uses solar power, in addition to battery power, to drive the electric motors [1-3]. Equally important as determining a new source of energy is the development of new materials that are both lightweight and of high strength. Previous literature [4-6] has investigated the mechanical properties of one such possible material: carbon nanotubes.

Comparing the specific surface energy of solar radiation and the current specific energy of batteries, it has been determined that they do not match the specific energy of gasoline. Because of this, battery-powered cars are still limited in the width and depth of applications. And, solar-powered cars have been somewhat restricted to academic applications.

Solar cars, such as the ones used in world solar challenges, require the building of an efficient system on all fronts (mechanical, aerodynamic, solar panels, batteries, etc.) in order to achieve high speeds and shortest travel times while simultaneously reducing the amount of energy consumed. The quest to improve on the efficiency of solar panels, and thus the energy produced by solar cars, has led to the investigation of space-based solar panels.

Alternatively, there is a special-application class of solar-battery cars that aims to minimize the use of battery power and maximize solar energy. One way to accomplish this is by increasing the size of the solar array. This paper explores the concept of using solar-trailers to increase the solar power input. This excess power is then used to drive accessories that, in some areas of the globe, may be necessary to life. When a solar-trailer is added to a system, the input solar energy is raised. However, this rise in energy may increase the influence of other factors as well, such as the weight of the car, drag and rolling resistances. In addition, this would lead to a reduction in the operating speed.

Thus, in order to justify the use of solar-trailers, the net power gained must be considerable and the reduction in speed must be justified. The solar power input, road profile, and type of application are a few of the parameters that may determine the preferred option. This paper explores the possibilities of using a car with solar-trailers. Initially, the energy consumed by a car alone, a car with one trailer, and a car with two trailers, is computed for a specific route. Next, the stability of the lateral dynamics is investigated using a linearized line model, for all three cases mentioned above. Analysis is completed by investigating the requirements for ground adhesion when travelling along a curved path.

The paper concludes with a preliminary evaluation of the suggested solar-battery car system with one/two solar-trailers. The appendix provides additional details regarding daily solar irradiance as measured and/or calculated on a horizontal surface,

and the power calculations for a solar trailer as a standalone entity.

II. ROAD DATA AND POWER CONSUMPTION OF BOTH A STANDALONE CAR AND A CAR WITH ONE/TWO SOLAR-TRAILERS

In this section, energy consumed by a single car is compared to that consumed by a car with one or two solar-trailers when driven during daylight hours, from 9:00AM to 5:00PM. The drive follows a simplified track at a latitude of 24.08°N, near the end of the month of March. The track is assumed to have a constant slope of 0.2%. The calculations are conducted at half-hour intervals with the effects of drag, gravity, rolling resistance and variable sunlight due to time change taken into account.

The method of computing the energy required to drive the track is based on a simplified approach [7]. The details of the various components of the car and trailers used in the analysis are as follows: the total mass of the car with passengers is 500kg, 300kg for the car and 200kg for passengers; this accounts for up to four passengers. Two masses for the trailer were tested: 100kg and 80kg. The efficiency of power conversion from input power to output power is assumed to be 85%. The power computations are described below:

a) Solar power: The maximum solar power, P_{\max} , per car or trailer, is assumed to be 1000W. The solar energy produced by the array while driving depends on the angle ϕ between the sunlight and the normal to the ground.

b) Aerodynamic force: For solar cars, the typical drag area AC_d is approximately 0.12m^2 [7, 8]. For a solar-battery car with up to four passengers, the aerodynamic force is calculated based on a drag area $AC_d = 3 \times 0.12\text{m}^2$ for the modified car. For the trailer, two values are considered: $AC_d = 0.12$ and 80% of 0.12. The drag area for a regular passenger car is approximately 5×0.12 . As far as the effect on drag due to the interaction between the car and trailers, this effect was reported in previous literature for airfoils in tandem [8]. Even though the distribution of drag coefficients altered, the resulting net effect on drag was small. Thus, this paper maintains drag area coefficients as specified above.

c) Rolling resistance: The rolling resistance for a solar car is approximately 0.005 [7]. Previous literature reported that the rolling resistance for a flat terrain varies between 0.0038 and 0.0054 for speeds of 40km/h and 90km/h, respectively [8]. In this paper, the rolling resistance coefficient for the wheels of the car is as assumed to be 0.01; the rolling resistance coefficient for the wheels of the trailer is assumed to be 0.0055.

d) Gravity resistance: The necessary power to overcome gravity resistance is determined by $P_{\text{gravity}} = \text{weight} \times \sin(\alpha) \times \text{speed}$ (W), where α is the angle of the inclined path. For small angles, α is assumed to be equal to the percentage of elevation. During the course of the day trip, the terrain is assumed to be almost flat with a percentage of elevation equal to 0.2%.

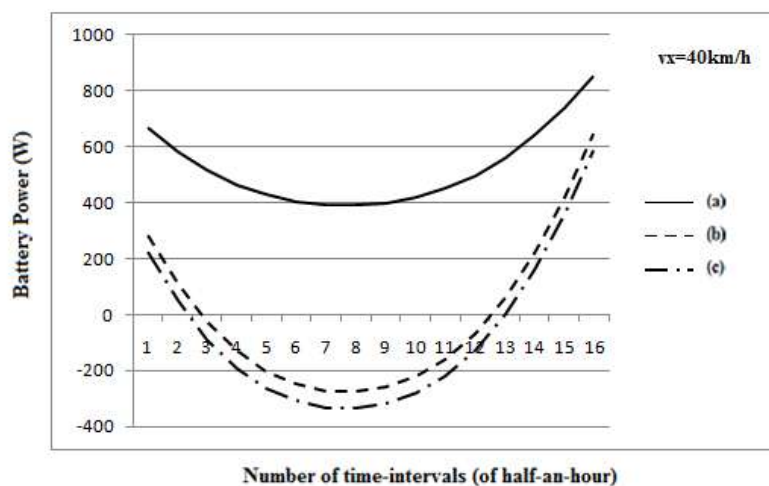
e) Necessary power: The total necessary power is obtained by adding the powers of drag, rolling resistance, and gravity: $P_{\text{drag}} + P_{\text{rolling}} + P_{\text{gravity}}$.

f) Battery power: The battery power required is equal to the power provided by the solar arrays subtracted from the total necessary power: $P_{\text{battery}} = (P_{\text{drag}} + P_{\text{rolling}} + P_{\text{gravity}}) - P_{\text{array}}$.

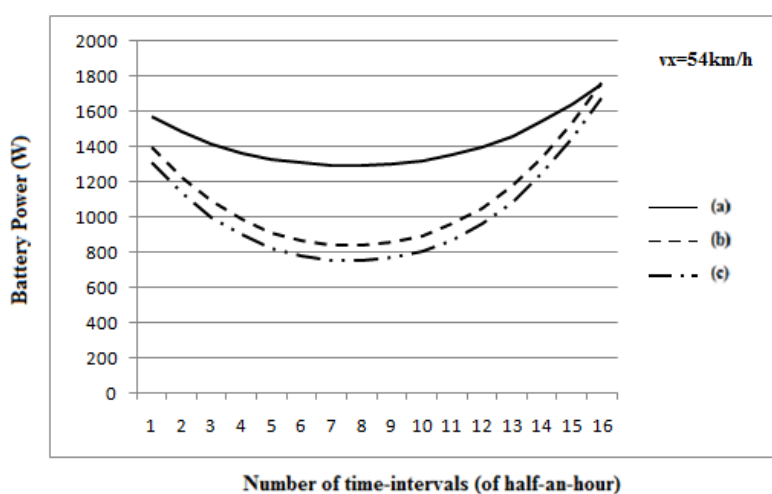
To begin, we calculate the battery power required to travel the specified track for a standalone car and a car with a single solar-trailer. Two different weights for the trailer were used, with two different drag coefficients. These three cases can be summarized as follows:

- (a) Car with a mass of 500kg.
- (b) Car with a trailer of mass 100kg and a drag area coefficient AC_d equal to 0.12.
- (c) Car with a trailer of mass 80kg and a drag area coefficient AC_d equal to 80% of 0.12.

The net battery power required during travel is calculated for the above three cases. Two speeds of travel were tested: 40km/h and 54km/h. The battery power required for each journey is plotted in Fig. 1 below. A negative battery power indicates excess power that can be stored in the battery.



(i)



(ii)

Fig. 1 Net battery power required for a multi-passengers car with and without one solar-trailer: (i) $V_x=40\text{km/h}$; (ii) $V_x=54\text{km/h}$

The procedure described above was applied to a standalone car and a car with two solar-trailers. Two different weights of trailer were used with two different drag coefficients, as follows:

- (a) Car with a mass of 500kg.
- (b) Car with two trailers of 100kg each and a drag area coefficient AC_d equal to 0.12.
- (c) Car with two trailers of 80kg each and a drag area coefficient AC_d equal to 80% of 0.12.

The battery power required for a car with and without two solar-trailers is plotted in Fig. 2. Results indicate that at a speed of 54km/h, cars with single and double solar-trailers rely on additional battery power to complete the journey; however, the car with two solar trailers would use considerably less battery power. Alternatively, at a speed of 40km/h, the car with a single solar-trailer may be able to travel with little reliance on battery power while the car with two solar-trailers would provide excess power to drive the accessories.

To complete the analysis, four other cases were investigated and summarized below:

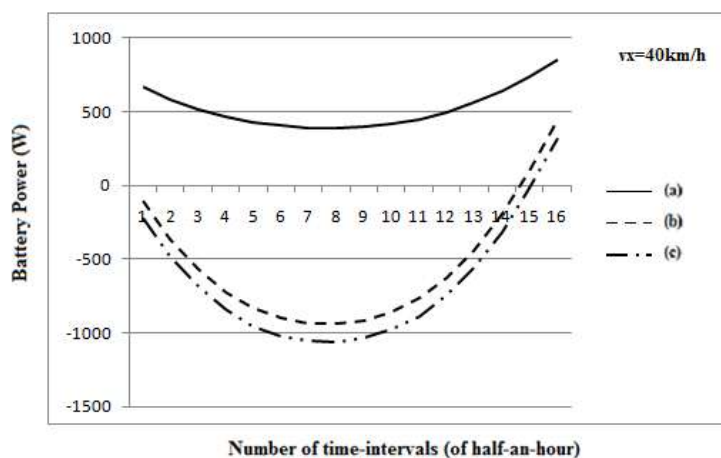
1) A multi-passenger car with two solar-trailers running at a speed of 70km/h; results are plotted in Fig. 3. Since the energy required is comparable to a single car, there is no benefit in using two solar-trailers at this speed.

2) A multi-passenger car with two solar-trailers running at a speed of 40km/h in mid-August. The average daily temperature is approximately 35°C, a rise of 10°C from previous cases. This rise in temperature results in a reduction of 50W in the maximum array power [7]. Energy versus time is plotted in Fig. 4. Still, similar energy savings are possible at this time of the year and at this speed.

3) A single-passenger car ($AC_d=0.12$) with two solar-trailers running at 40km/h. As expected, considerable energy saving is possible, as shown in Fig. 5.

4) A single-passenger car ($AC_d=0.12$) with two solar-trailers running at 70km/h. Although some battery energy saving is possible, the limit of solar-trailer applicability is approached, as presented in Fig. 6.

In conclusion, for single- and multi-passenger(s) cars running on a track as described above at a speed near 40km/h, excess solar energy could be harvested throughout the year, with little or no reliance on battery power.



(i)

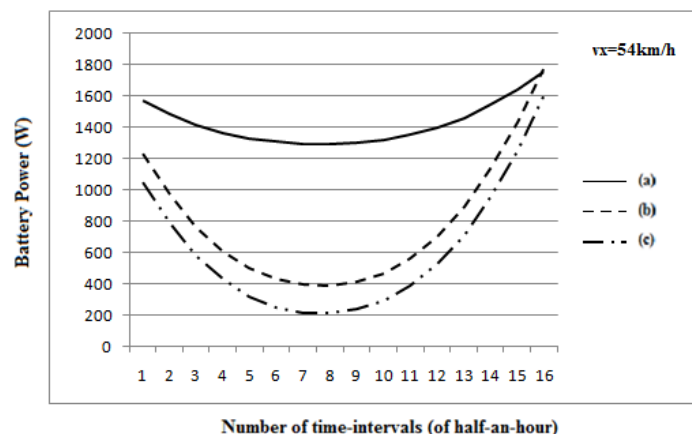


Fig. 2 Net battery power required for multi-passenger car with and without two solar-trailers:

(i) $V_x=40\text{km/h}$; (ii) $V_x=54\text{km/h}$

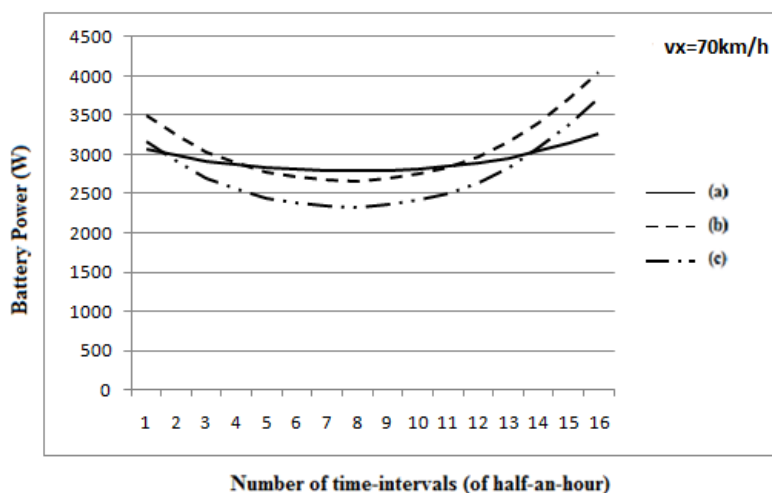


Fig. 3 Net battery power required for a multi-passenger car with or without two solar-trailers

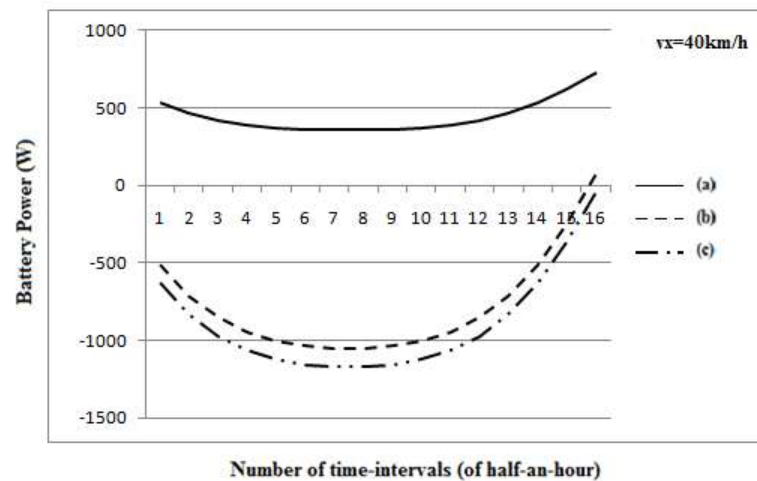


Fig. 4 Net battery power required for a multi-passenger car with or without two solar-trailers in mid-August

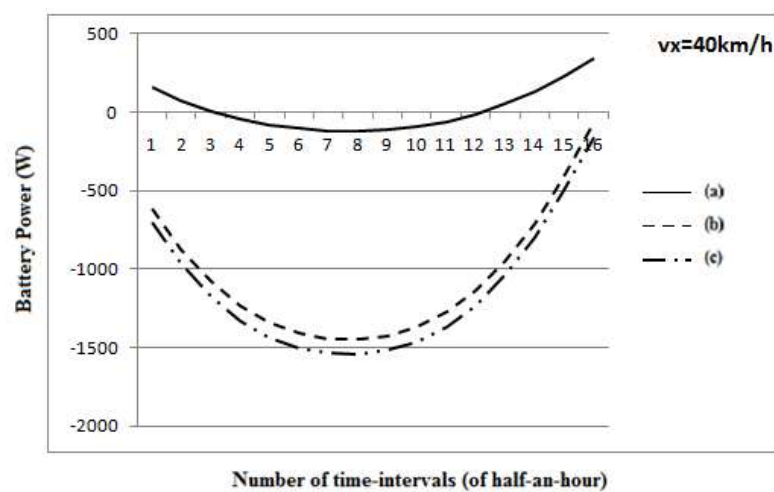


Fig. 5 Net battery power required for a single-passenger car with or without two solar-trailers

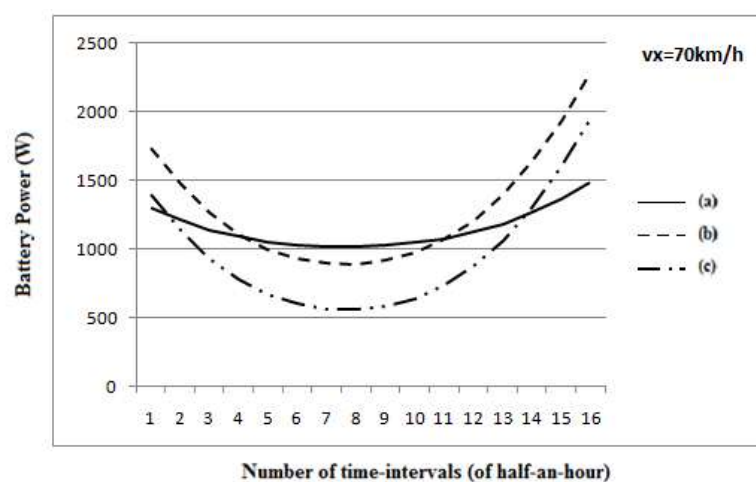


Fig. 6 Net battery power required for a single-passenger car with or without two solar-trailers

III. LINEARIZED EQUATIONS OF MOTION OF A SOLAR-BATTERY CAR WITH SINGLE/DOUBLE SOLAR-TRAILERS

To study the dynamics of cars, one approach is to numerically integrate the three-dimensional equations of motion [9-11]. However, in order to simplify the procedure for preliminary analysis, the idealization of a line model may be useful [12-14]. The line model of a solar-battery car with two solar-trailers is shown in Fig. 7, below.

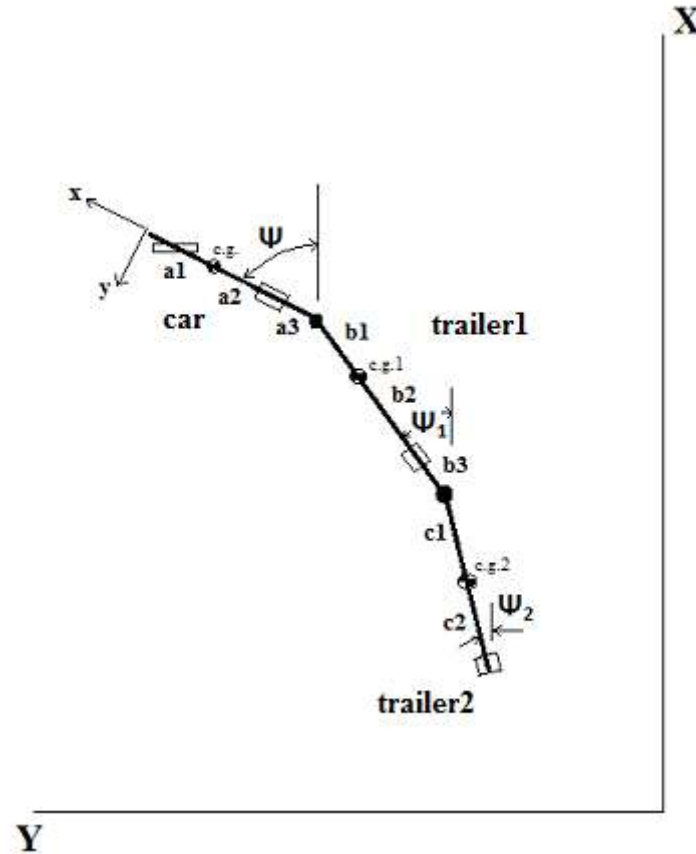


Fig. 7 Line model of a solar-battery car with two solar-trailers

Using linearization of the equations, the accelerations, lateral forces, and equations of motion of the car and the two trailers for small angular rotations can be written as shown below. The nomenclature is described in Table 1.

A. Accelerations

$$a_y = \dot{v}_y + \omega * vx; \quad (1)$$

$$a_{y1} = \dot{v}_y - (a_2 + a_3 + b_1) * \dot{\omega} + b_1 * \ddot{\theta} + \omega * vx; \quad (2)$$

$$a_{y2} = \dot{v}_y - (a_2 + a_3 + b_1 + b_2 + b_3 + c_1) * \dot{\omega} + (b_1 + b_2 + b_3 + c_1) * \ddot{\theta} + c_1 * \ddot{\alpha} + \omega * vx; \quad (3)$$

B. Lateral Forces

$$F_{yf} = caf * (\delta - (v_y + a_1 * \omega) / v_x); \quad (4)$$

$$F_{yr} = -car * (v_y - a_2 * \omega) / v_x; \quad (5)$$

$$F_{yr1} = -car_1 * (v_y - (a_2 + a_3 + b_1 + b_2) * \omega + (b_1 + b_2) * \dot{\theta} + vx * \dot{\theta}) / v_x; \quad (6)$$

where $a_{23}=a_2+a_3$, $b=b_1+b_2+b_3$ and $c_{12}=c_1+c_2$. Thus, we obtain:

$$F_{yr2} = -car_2 * (v_y - (a_{23} + b + c_{12}) * \omega - (b + c_{12}) * \dot{\theta} + c_{12} * \ddot{\alpha} + vx * \dot{\theta} + vx * \ddot{\alpha}) / v_x; \quad (7)$$

C. C. Linearized equations of motion (neglecting product terms) [12-14]

1) Car:

$$m^* ay = F_{yf} + F_{yr} + T_y; \quad (8)$$

$$I_z \dot{\omega} = F_{yf} * a_1 - F_{yr} * a_2 - T_y * (a_2 + a_3) \quad (9)$$

2) *Trailer 1:*

$$m_1^* ay_1 = F_{yr1} + S_y - T_y; \quad (10)$$

$$I_{z1} \dot{\omega}_1 = -F_{yr1} * b_2 - S_y * (b_2 + b_3) - T_y * b_1 \quad (11)$$

3) *Trailer 2:*

$$m_2^* ay_2 = F_{yr2} - S_y; \quad (12)$$

$$I_{z2} \dot{\omega}_2 = -F_{yr2} * c_2 - S_y * c_1 \quad (13)$$

TABLE 1 NOMENCLATURE FOR LINE MODEL OF A CAR WITH TRAILERS

a_1, a_2, a_3	Distance from the front wheel of the car to the center of gravity (c.g.), and c.g. to the rear wheel, and from the rear wheel to the trailer1 connection, respectively.
b_1, b_2, b_3	Distance from the connection to the c.g. of trailer1, from c.g. 1 to the rear wheel, and from the rear wheel to the connection with trailer 2, respectively.
c_1, c_2	Distance from the connection to c.g. 2 of trailer 2, and from c.g. 2 to the rear wheel, respectively.
a_y, a_{y1}, a_{y2}	The y-accelerations of the car, trailer 1 and trailer 2, respectively.
Ψ, Ψ_1, Ψ_2	The angle between the X-axis and the x-axes of the car, trailer 1 and trailer 2, respectively.
v_x, v_y	The x- and y-velocities of the car.
θ	$\Psi - \Psi_1$
α	$\Psi_2 - \Psi_1$
δ	Front wheel steering angle.
ω	$d\Psi/dt$
m, m_1, m_2	Masses of the car, trailer 1 and trailer 2, respectively.
I_z, I_{z1}, I_{z2}	Mass moments of inertia along the z-axis of the car, trailer 1 and trailer 2, respectively.
F_{yf}, F_{yr}	Lateral front and rear forces of the car.
T_x, T_y	The car-trailer 1 connection forces along the x- and y-directions.
S_x, S_y	The trailer 1-trailer 2 connection forces along the x- and y-directions.
$c_{af, car}$	Lateral stiffness coefficients of the front and rear wheels of the car.

IV. STABILITY OF THE LATERAL DYNAMICS USING A LINEARIZED LINE MODEL

The equations of motion, rearranged as matrices, can be written as follows:

$$A(dx/dt) + Bx = C(\delta(t)), \quad (14)$$

where the vector \mathbf{x} is given by $\mathbf{x} = [v_y \ \omega \ \theta \ \alpha \ d\theta/dt \ d\alpha/dt]^T$. In the absence of a steering input $\delta(t)$, the system of equations reduces to:

$$dx/dt + A^{-1}Bx = 0, \quad (15)$$

If $D = -A^{-1}B$, then:

$$dx/dt = Dx, \quad (16)$$

For such a system to be stable, the eigenvalues of D must represent negative real values [12-14]. These equations will be used to calculate the eigenvalues of the system described above for a car with one or two solar-trailers. The properties of the car and trailers used in the analyses are shown in Table 2. The cornering stiffness is assumed to depend on the vertical load and

the slip, as derived by Roland [8].

TABLE 2 PROPERTIES OF THE CAR AND TRAILERS

	mass (kg)	Iz (kg.m ²)	a ₁ /b ₁ /c ₁ (m)	a ₂ /b ₂ /c ₂ (m)	a ₃ /b ₃ (m)	Two trailers caf/car (N/rad.)	Single trailer caf/car (N/rad.)
Car	500.	600.	1.5	1.5	0.5	2.*6581./ 2.*5748.	2.*6590./ 2.*5604.
Trailer 1	80.	100.	2.2	1.8	0.5	2.*4477.	2.*2622.
Trailers 1 and 2	80./80.	100./100	2.2	1.8		2.*2622.	

Three speeds were tested: $v_x=40\text{km/h}$, 54km/h and 80km/h . The resulting eigenvalues of a car with one and two solar-trailers are listed in Tables 3, 4 and 5.

TABLE 3 EIGENVALUES OF A CAR WITH ONE AND TWO SOLAR-TRAILER(S) AT A SPEED OF $V_x=40\text{km/h}$

	Eigen 1	Eigen 2	Eigen 3	Eigen 4	Eigen 5	Eigen 6
Car+trailer 1	-1.738	-4.794	-9.029	-12.405		
Car+trailers 1 and 2	-2.409	-3.342+0.641i	-3.342-0.641i	-9.166	-9.542	-17.827

TABLE 4 EIGENVALUES OF A CAR WITH ONE AND TWO SOLAR-TRAILER(S) AT A SPEED OF $V_x=54\text{km/h}$

	Eigen 1	Eigen 2	Eigen 3	Eigen 4	Eigen 5	Eigen 6
Car+trailer 1	-0.824	-6.340+3.751i	-6.340-3.751i	-7.209		
Car+trailer 1 and 2	-1.107	-3.411+2.773i	-3.411-2.773i	-7.173	-9.346+4.792i	-9.346-4.792i

TABLE 5 EIGENVALUES OF A CAR WITH ONE AND TWO SOLAR-TRAILER(S) AT A SPEED OF $V_x=80\text{km/h}$

	Eigen 1	Eigen 2	Eigen 3	Eigen 4	Eigen 5	Eigen 6
Car+trailer 1	0.272	-4.244+5.830i	-4.244-5.830i	-5.767		
Car+trailer 1 and 2	0.055	-2.452+3.961i	-2.452-3.961i	-5.672	-6.146+7.675i	-6.146-7.675i

As expected, decreasing speed increases the stability of both systems by increasing the damping. For a car with one solar trailer at a speed of 40km/h , the eigenvalues of the system are all real and negative; thus, the system is stable. At a speed of 54km/h , although all eigenvalues have negative real parts, some eigenvalues are complex-conjugate; consequently, the system is oscillatory but still damped.

For the car with two solar-trailers at speeds of 40km/h and 54km/h , the eigenvalues have negative real parts but are complex-conjugate; this results in an oscillatory but stable system. At a speed of 80km/h , both configurations have already entered the unstable regime.

For the current geometries, the behavior of the car alone is neutral steer [13, 14]. For the car with a single trailer, the response is oversteer. Using the closed form expression for the critical speed, as developed in previous literature [14], a value of 71.8km/h can be calculated as the limiting speed of stability. Thus, a speed of 80km/h would exceed the comfort zone for these systems, as predicted in Table 5.

V. GROUND FORCES DEVELOPED WHEN TRAVELING ALONG A CURVE

The ground forces necessary to travel along a curve at high speeds may exceed the forces that could develop between the tire and the ground. This section investigates the ground forces needed for a speed of 40km/h at two steering angles: 2.86° (0.05rad) and 4.58° (0.08rad).

For a steering angle of 2.86° , the steady state radius traveled is 44.3m , as shown in Fig. 8(a). Alternatively, for a steering angle of 4.58° , the steady state radius traveled is 27.7m , as shown in Fig. 8(b). At low speeds, Ackerman radius can be utilized as a limiting case. The steady state radius for a slow moving car at 3.6km/h is $R=59.9\text{m}$, as shown in Fig. 8(c). The calculated radius based on the Ackerman equations is 60m for a steering angle of 0.05rad .

The ground “friction” coefficients, relating the horizontal forces to the vertical forces developed at the ground, are plotted in Figs. 9(a) and 9(b), respectively. Although the “friction” coefficients are higher in the second case due to the smaller turning radius, and produce consequently higher lateral accelerations, their values are still within the limits for dry asphalt surfaces [15].

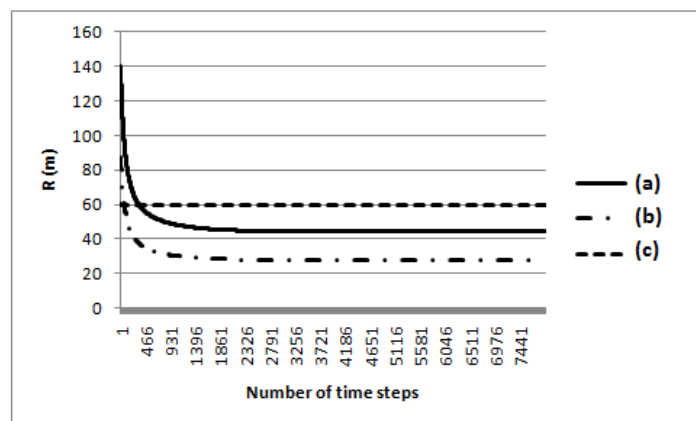
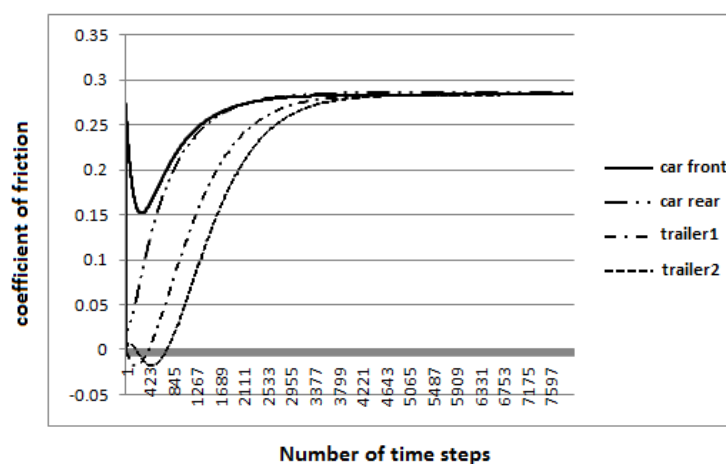
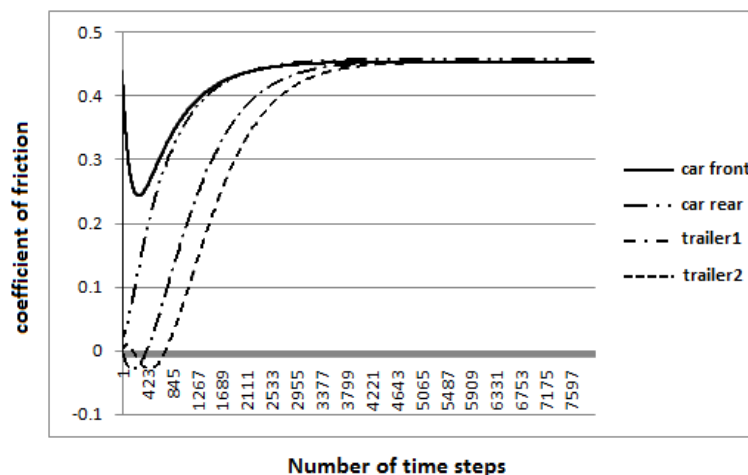


Fig. 8 Radius of Curvature R vs. number of time steps:

(a) Steering input $\delta=0.05\text{rad}$, $V_x=40\text{km/h}$; (b) $\delta=0.08\text{rad}$, $V_x=40\text{km/h}$; (c) $\delta=0.05\text{rad}$, $V_x=3.6\text{km/h}$



(a)



(b)

Fig. 9 Coefficients of friction vs. number of time steps and steering input (a) $\delta=0.05\text{rad}$; (b) $\delta=0.08\text{rad}$

VI. CONCLUSIONS

This paper explored the concept of using solar-trailers for a specialized class of solar cars. This concept may apply to regions of the globe where solar energy is abundant. The power calculations indicated that there is a significant net power produced by systems using two solar-trailers. At a speed of 54km/h, cars with one and two solar-trailers would rely on additional battery power to complete the journey. However, a car with two solar-trailers would use considerably less battery power. Alternatively, at a speed of 40km/h, a car with a single solar-trailer may be able to travel with little reliance on battery power. However, the car with two solar-trailers would provide excess power to drive the accessories. In addition, preliminary

calculations demonstrated that at moderate speeds, the lateral dynamics are stable and the ground forces developed are within acceptable boundaries.

APPENDIX

In this appendix, daily distribution of solar irradiance is compared as measured at a Solar Station, at the Royal Commission-Yanbu in Saudi Arabia, and the calculated value based on the employed method [7]. In addition, power requirements for a standalone solar-trailer are calculated, and the limits on the adopted physical parameters are discussed.

A. Daily Solar Irradiance on a Horizontal Plane: Measured vs. Calculated

It is well known that an average of 1367 W/m^2 of specific solar power hits the outside atmosphere of the Earth, on a daily basis [16]; an estimated 30% is lost due to absorption and scattering. Thus, this paper assumes that the maximum solar irradiance hitting a horizontal ground surface is 1000 W/m^2 . Based on this value of solar irradiance, the calculated daily distribution from sunrise to sunset on July 22nd, 2015, is plotted in Fig. 10.

The King AbdulLah City for Atomic and Renewable Energy (K. A.CARE) publishes daily solar irradiance data for various stations in Saudi Arabia, in addition to other important matters [17]. The online data for the Global Horizontal Solar Irradiance for the 22nd of July, 2015, as measured on a horizontal plane at the Yanbu Royal Commission Station, is reproduced in Fig. 10. Comparison of the above two plots reveals that the relative error between the measured raw solar irradiance data and the calculated value, based on the equation discussed above, varies from -9.5% to 4.9% between 10AM and 3PM, and from -31.5% to 4.9% between 9AM and 5PM. Further analysis might use the available data from K.A. CARE to perform a more detailed analysis over a longer period of time.

B. Power Calculations for a Solar-Trailer as a Standalone Entity

The following will provide more details on the power calculations, the suitability of the parameters chosen, and the resulting benefits of using a solar trailer.

A solar trailer may be considered as a subset of a solar car without the driver, battery, wheel(s) and electric motor. In the above analyses, two weights were used to represent the solar trailer: 80kg and 100kg. Additionally, two values for the drag area coefficient were selected: 0.12 m^2 and 80% of 0.12 m^2 . Analysis of the solar car known as the “The Shark” [10], by eliminating the components that are not common in solar-trailers, reveals that the physical properties are similar to those of the solar-trailer in the analyses. Additionally, solar power savings are still possible by adopting advances in technology, as presented in previous literature [18-21].

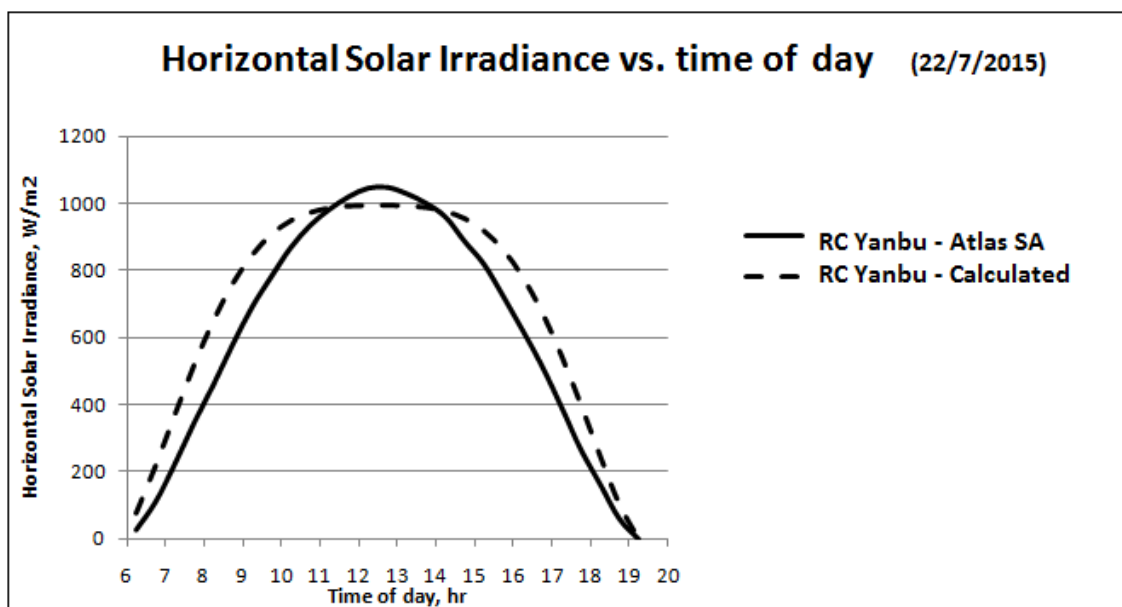


Fig. 10 Horizontal solar irradiance vs time of day

With regard to the road profile, the application is assumed to occur on a nearly flat surface with a gradient of approximately 0.2%.

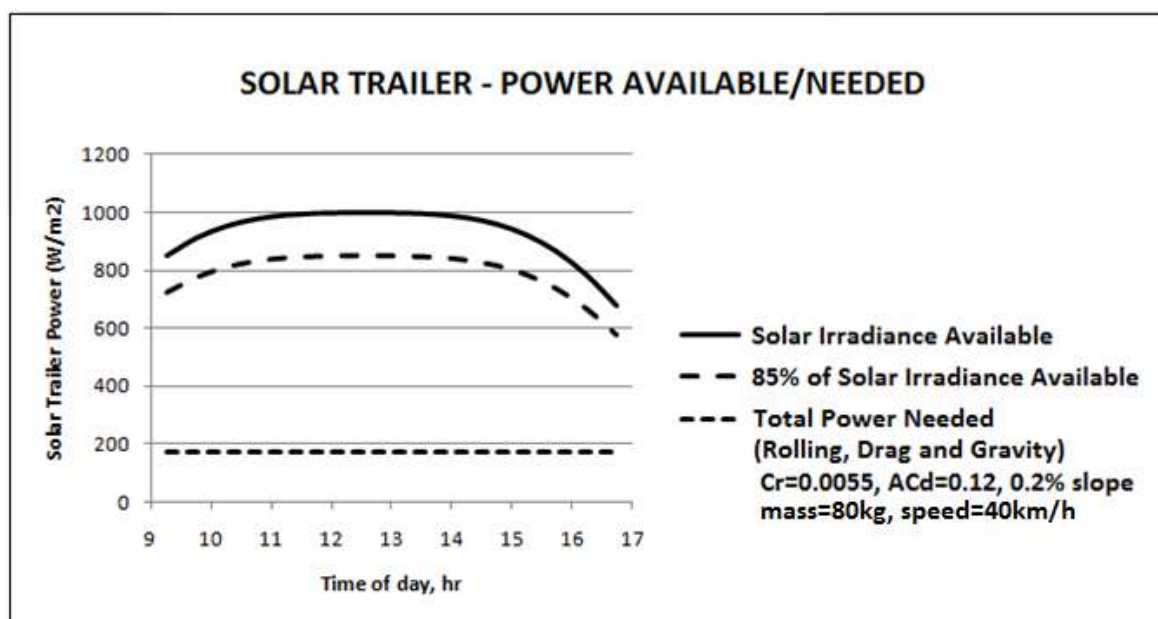


Fig. 11 Solar-trailer power as available and required

As far as the solar panels, a specific power of 1000W/m^2 is assumed to be incident on an area of 8m^2 of solar panels (approximately $2\text{m} \times 4\text{m}$) with 12.5% efficiency. This leads to the production of 1000W/m^2 per set of panels, on the car and solar-trailers.

The use of more efficient panels will lead to greater power production, and thus, greater savings of battery power than the values predicted above. Doubling the solar panels' efficiency is possible [21].

Fig. 11 compares the specific energy produced by a set of panels on the solar-trailer, the useful mechanical power available from these panels (assuming 85% mechanical efficiency), and the total power used to overcome drag, rolling resistance and gravity. This plot shows the net power available with the addition of a solar-trailer, irrespective of the solar car used.

REFERENCES

- [1] CALSOL, UC Berkeley Solar Vehicle.
- [2] ELEANOR, MIT Solar Electric Vehicle.
- [3] STELLA, Solar-powered family car by TU Eindhoven.
- [4] Kasti, N., *Carbon Nanotubes under Simple Tension and Torsion Molecular/Structural Mechanics and the Finite Element Method*, Physical and Chemical Properties of Carbon Nanotubes, Dr. Satoru Suzuki (Ed.), ISBN: 978-953-51-1002-6, InTech, 2013.
- [5] Kasti N., "Zigzag Carbon Nanotubes under Simple Torsion – Structural Mechanics Formulation," *Advanced Materials Research*, vol. 452-453, pp. 1139-1143, 2012.
- [6] Kasti, N., "Zigzag Carbon Nanotube: Molecular/Structural Mechanics and the Finite Element Method", *International Journal of Solids and Structures*, vol. 44, Iss. 21, pp. 6914-6929, 2007.
- [7] Carrol, R., *The Winning Solar Car*, SAE International, 2003.
- [8] Thacher, E., *A Solar Car Primer*, Nova Science Publishers, 2010.
- [9] Gerardin, M. and Cardona A., *Flexible Multibody Dynamics: A Finite Element Approach*, John Wiley & Sons, 2001.
- [10] Haug E., *Computer-Aided Kinematics and Dynamics of Mechanical Systems*, vol. I, Allyn and Bacon, 1989.
- [11] Kasti, N., "A Numerical Integration Scheme for the Dynamic Motion of Rigid Bodies using the Euler parameters", *International Journal of Research in Engineering and Science*, vol. 2, no. 8, pp. 30-38, 2014.
- [12] Hac, A., Fulk, D., and Chen, H., "Stability and Control Considerations of Vehicle-Trailer Combination", SAE Technical paper 2008-01-1228.
- [13] Jazzar, R., *Vehicle Dynamics: Theory and Applications*, Springer, 2008.
- [14] Ellis, J. R., *Vehicle Dynamics*, Business Books Limited, 1969.
- [15] Vehicle Dynamics, Chap. 4. [Online]. Available: http://scholar.lib.vt.edu/theses/available/etd-5440202339731121/unrestricted/CHAP3_DOC.pdf.
- [16] Part2: Solar Energy Reaching the Earth's Surface. [Online]. Available: <http://www.itacanet.org/the-sun-as-a-source-of-energy/part-2-solar-energy-reaching-the-earths-surface/>.
- [17] The King AbdulLah City for Atomic and Renewable Energy (K.A.CARE). [Online]. Available: <https://rratlas.kacare.gov.sa/RRMMPublicPortal/?q=en>.

- [18] Michelin Media Information, World Solar Challenge, 2013.
- [19] Frydrychowicz-Jastrzebska, G., Gomez, E. Perez, Computer Simulation of Power Balance of a Solar Vehicle depending on its Parameters and Outside Factors.
- [20] Designing a Revolutionary Solar Electric Vehicle, University of Cambridge, ASWC 2013.
- [21] Ozawa, H., Nishikawa, S., and Higashida, D., "Development of Aerodynamics for a Solar Race Car," *Society of Automotive Engineers of Japan*, vol. 19, pp. 343-349, 1998.